Conserved charges in the real-device quantum simulation of integrable spin chains

Takuya Okuda, University of Tokyo, Komaba

Based on J.Phys.A 56 (2023) 16, 165301 (arXiv:2208.00576)
with Kazunobu Maruyoshi, Juan William Pedersen, Ryo Suzuki, Masahito Yamazaki, Yutaka Yoshida

Plan of the talk

- Motivations and background
- Integrable Trotterization of XXX spin chain
- Quantum devices
- Simulation results/theoretical analysis
- Summary and future directions

Motivations and background

- The simulation of lattice gauge theories and more general quantum many-body systems is expected to become a major target of application of quantum computers in the future.
- We should be preparing
  - by developing the theory of quantum simulation and
  - by **implementing quantum algorithms on the available real devices**.

- Currently, we only have noisy intermediate-scale quantum (NISQ) devices. Their abilities are limited by noise (errors) and size.
  - Q1: Can we quantify the effects of **quantum noise** using a many-body system?
  - Q2: Is there a way to put **discretization errors** under control?

- Because the realistic lattice gauge theories (such as lattice QCD) are hard to simulate on current devices, we consider a spin chain as a toy model.
- It is generally expected that integrable models provide useful benchmarks for quantum simulation because they allow greater analytical control, even when the system size is so large that classical simulation is impossible.
- Today I report the results of our quantum simulation of the Heisenberg spin 1/2 XXX spin chain on real devices.
  - Trapped-ion device (IonQ)
  - Superconducting devices (IBM)

Integrable Trotterization

Integrable Trotterization

[Vanicat, Zadnik & Prosen '17]

- XXX Hamiltonian:

$$H \propto \sum_{j=1}^{N} \boldsymbol{\sigma}_j \cdot \boldsymbol{\sigma}_{j+1} = H_e + H_o \,.$$

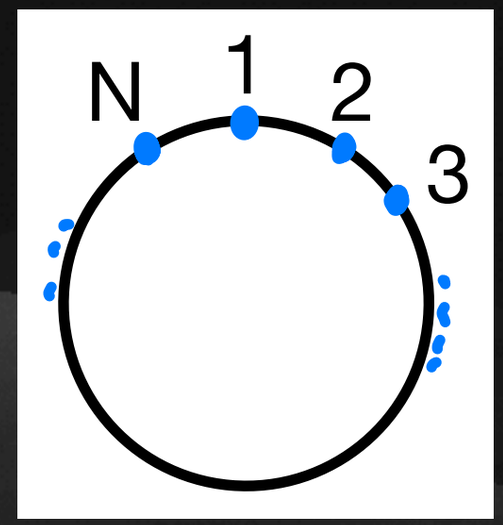

$$\boldsymbol{\sigma} \equiv (\sigma_x, \sigma_y, \sigma_z) \equiv (X, Y, Z)$$

- Ideally, we want to implement e^{-itH}. This is not possible and we resort to the Suzuki-Trotter **approximation**

$$(e^{-i(t/d)H_e} e^{-i(t/d)H_o})^d = e^{-it(H_e+H_o)}(1 + \mathcal{O}(d^{-1}))\,.$$

d: number of repetitions $\sim$ depth

The Trotterized small-time evolution (even N, periodic b.c.) can be expressed in terms of the R(-check) matrix:

$$e^{-i\alpha H_e}e^{-i\alpha H_o} = \left(\prod_{j=1}^{N/2} R_{2j-1,2j}(\delta)\right)\left(\prod_{j=1}^{N/2} R_{2j,2j+1}(\delta)\right) =: \mathcal{U}(\delta)\,,$$

$$R_{ij}(\delta) = (1 + i\delta P_{ij})/(1 + i\delta)$$
$$= (\text{phase})e^{i\alpha(X_iX_j+Y_iY_j+Z_iZ_j)}\,.$$

$$(\delta = \tan\alpha)$$

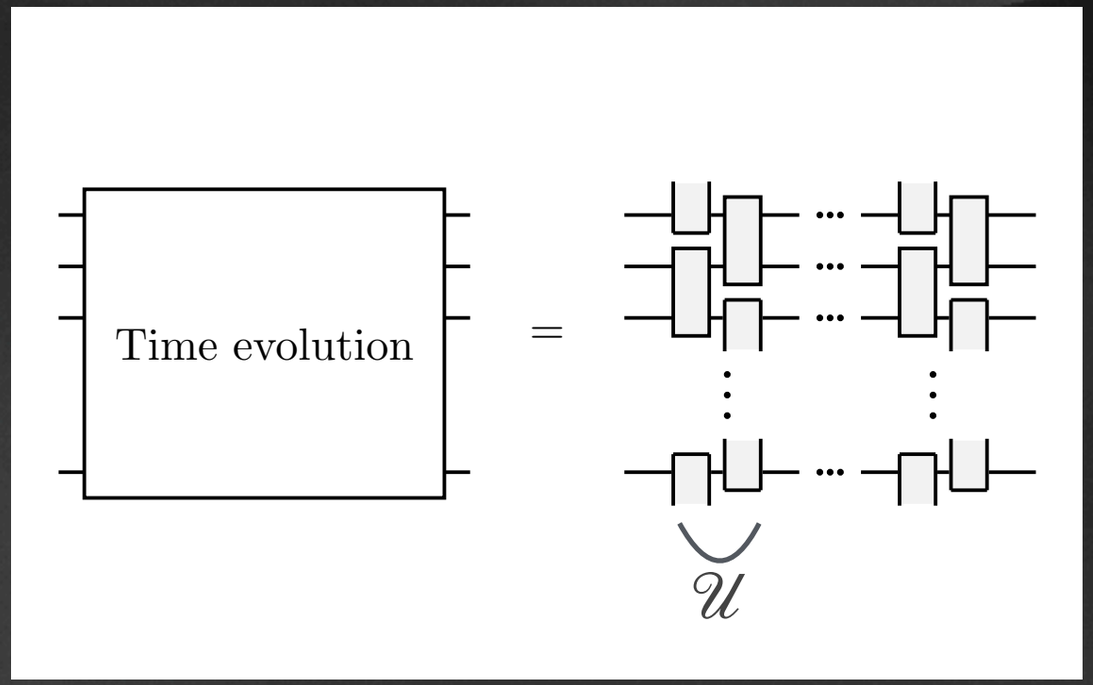

Conserved charges

- $\mathcal{U}(\delta)$ commutes with the transfer matrix with specific inhomogeneity

$$T_\delta(\lambda) = \mathrm{tr}_0\left[\overleftarrow{\prod_{1\le j\le N}} R_{0j}\left(\lambda - (-1)^j\delta\right)\right] \text{ for any } \lambda \in \mathbb{C}.$$

- Charges $Q_n^{\pm}(\delta) \sim \dfrac{d^n}{d\lambda^n}\log T_\delta(\lambda)\Big|_{\lambda=\pm\delta/2}$ are **exactly conserved** even with Trotterization, which give rise to time-discretization errors for other observables.

- $Q_n^{\mathrm{dif}} \equiv [Q_n^{+}(\delta) - Q_n^{-}(\delta)]/\delta$ is also conserved.

- Densities $q^{[n,\pm]}_{j,j+1,\ldots,j+2n}$ in higher charges

$$Q^{+}_{n}(\delta) = \sum_{j=1}^{N/2} q^{[n,+]}_{2j-2,2j-1,\ldots,2j+2n-2}(\delta)\,,$$

$$Q^{-}_{n}(\delta) = \sum_{j=1}^{N/2} q^{[n,-]}_{2j-1,2j,\ldots,2j+2n-1}(\delta)$$

can be computed via the recursion relation $Q^{\pm}_{n+1} \sim [B, Q^{\pm}_{n}]$ on an infinite chain, where B is a discrete (Lorentz) boost transformation. [Vanicat et al.]

- We implemented the recursion in Mathematica programs.

known

new

$$
\begin{aligned}
q^{[1,\pm]}_{1,2,3}(\delta) &= \boldsymbol{\sigma}_1\cdot\boldsymbol{\sigma}_2+\boldsymbol{\sigma}_2\cdot\boldsymbol{\sigma}_3\mp\delta\boldsymbol{\sigma}_1\cdot(\boldsymbol{\sigma}_2\times\boldsymbol{\sigma}_3)+\delta^2\boldsymbol{\sigma}_2\cdot\boldsymbol{\sigma}_3\,,\\
q^{[2,\pm]}_{1,2,3,4,5}(\delta) &= \mp2\delta(\boldsymbol{\sigma}_3\cdot\boldsymbol{\sigma}_4+\boldsymbol{\sigma}_4\cdot\boldsymbol{\sigma}_5-\boldsymbol{\sigma}_3\cdot\boldsymbol{\sigma}_5)-(1-\delta^2)\boldsymbol{\sigma}_3\cdot(\boldsymbol{\sigma}_4\times\boldsymbol{\sigma}_5)-\boldsymbol{\sigma}_2\cdot(\boldsymbol{\sigma}_3\times\boldsymbol{\sigma}_4)-\delta^2\boldsymbol{\sigma}_2\cdot(\boldsymbol{\sigma}_3\times\boldsymbol{\sigma}_5)\\
&\quad-\delta^2\boldsymbol{\sigma}_1\cdot(\boldsymbol{\sigma}_3\times\boldsymbol{\sigma}_4)-\delta^4\boldsymbol{\sigma}_1\cdot(\boldsymbol{\sigma}_3\times\boldsymbol{\sigma}_5)\pm\delta\boldsymbol{\sigma}_2\cdot(\boldsymbol{\sigma}_3\times\boldsymbol{\sigma}_4\times\boldsymbol{\sigma}_5)\pm\delta\boldsymbol{\sigma}_1\cdot(\boldsymbol{\sigma}_2\times\boldsymbol{\sigma}_3\times\boldsymbol{\sigma}_4)\\
&\quad\pm\delta^3\boldsymbol{\sigma}_1\cdot(\boldsymbol{\sigma}_3\times\boldsymbol{\sigma}_4\times\boldsymbol{\sigma}_5)\pm\delta^3\boldsymbol{\sigma}_1\cdot(\boldsymbol{\sigma}_2\times\boldsymbol{\sigma}_3\times\boldsymbol{\sigma}_5)-\delta^2\boldsymbol{\sigma}_1\cdot(\boldsymbol{\sigma}_2\times\boldsymbol{\sigma}_3\times\boldsymbol{\sigma}_4\times\boldsymbol{\sigma}_5)\,,\\
q^{[3,+]}_{1,2,3,4,5,6,7} &= -4\boldsymbol{\sigma}_6\cdot\boldsymbol{\sigma}_7+2\boldsymbol{\sigma}_5\cdot\boldsymbol{\sigma}_7-4\boldsymbol{\sigma}_5\cdot\boldsymbol{\sigma}_6+2\boldsymbol{\sigma}_4\cdot\boldsymbol{\sigma}_6+2\boldsymbol{\sigma}_4\cdot(\boldsymbol{\sigma}_5\times\boldsymbol{\sigma}_6\times\boldsymbol{\sigma}_7)+2\boldsymbol{\sigma}_3\cdot(\boldsymbol{\sigma}_4\times\boldsymbol{\sigma}_5\times\boldsymbol{\sigma}_6)\\
&\quad+\delta\Big(10\boldsymbol{\sigma}_5\cdot(\boldsymbol{\sigma}_6\times\boldsymbol{\sigma}_7)-2\boldsymbol{\sigma}_4\cdot(\boldsymbol{\sigma}_6\times\boldsymbol{\sigma}_7)-4\boldsymbol{\sigma}_4\cdot(\boldsymbol{\sigma}_5\times\boldsymbol{\sigma}_7)+8\boldsymbol{\sigma}_4\cdot(\boldsymbol{\sigma}_5\times\boldsymbol{\sigma}_6)-4\boldsymbol{\sigma}_3\cdot(\boldsymbol{\sigma}_5\times\boldsymbol{\sigma}_6)\\
&\quad-2\boldsymbol{\sigma}_3\cdot(\boldsymbol{\sigma}_4\times\boldsymbol{\sigma}_6)-4\boldsymbol{\sigma}_3\cdot(\boldsymbol{\sigma}_4\times\boldsymbol{\sigma}_5\times\boldsymbol{\sigma}_6\times\boldsymbol{\sigma}_7)-2\boldsymbol{\sigma}_2\cdot(\boldsymbol{\sigma}_3\times\boldsymbol{\sigma}_4\times\boldsymbol{\sigma}_5\times\boldsymbol{\sigma}_6)\Big)\\
&\quad+\delta^2\Big(2\boldsymbol{\sigma}_6\cdot\boldsymbol{\sigma}_7-10\boldsymbol{\sigma}_5\cdot\boldsymbol{\sigma}_7+2\boldsymbol{\sigma}_5\cdot\boldsymbol{\sigma}_6+2\boldsymbol{\sigma}_4\cdot\boldsymbol{\sigma}_7+2\boldsymbol{\sigma}_4\cdot\boldsymbol{\sigma}_6+2\boldsymbol{\sigma}_3\cdot\boldsymbol{\sigma}_6\\
&\quad-6\boldsymbol{\sigma}_4\cdot(\boldsymbol{\sigma}_5\times\boldsymbol{\sigma}_6\times\boldsymbol{\sigma}_7)+6\boldsymbol{\sigma}_3\cdot(\boldsymbol{\sigma}_5\times\boldsymbol{\sigma}_6\times\boldsymbol{\sigma}_7)+2\boldsymbol{\sigma}_3\cdot(\boldsymbol{\sigma}_4\times\boldsymbol{\sigma}_6\times\boldsymbol{\sigma}_7)+6\boldsymbol{\sigma}_3\cdot(\boldsymbol{\sigma}_4\times\boldsymbol{\sigma}_5\times\boldsymbol{\sigma}_7)\\
&\quad-6\boldsymbol{\sigma}_3\cdot(\boldsymbol{\sigma}_4\times\boldsymbol{\sigma}_5\times\boldsymbol{\sigma}_6)+2\boldsymbol{\sigma}_2\cdot(\boldsymbol{\sigma}_3\times\boldsymbol{\sigma}_5\times\boldsymbol{\sigma}_6)\\
&\quad+2\boldsymbol{\sigma}_2\cdot(\boldsymbol{\sigma}_3\times\boldsymbol{\sigma}_4\times\boldsymbol{\sigma}_5\times\boldsymbol{\sigma}_6\times\boldsymbol{\sigma}_7)+2\boldsymbol{\sigma}_1\cdot(\boldsymbol{\sigma}_2\times\boldsymbol{\sigma}_3\times\boldsymbol{\sigma}_4\times\boldsymbol{\sigma}_5\times\boldsymbol{\sigma}_6)\Big)\\
&\quad+\delta^3\Big(6\boldsymbol{\sigma}_5\cdot(\boldsymbol{\sigma}_6\times\boldsymbol{\sigma}_7)-2\boldsymbol{\sigma}_4\cdot(\boldsymbol{\sigma}_6\times\boldsymbol{\sigma}_7)+4\boldsymbol{\sigma}_4\cdot(\boldsymbol{\sigma}_5\times\boldsymbol{\sigma}_7)-2\boldsymbol{\sigma}_3\cdot(\boldsymbol{\sigma}_6\times\boldsymbol{\sigma}_7)-8\boldsymbol{\sigma}_3\cdot(\boldsymbol{\sigma}_5\times\boldsymbol{\sigma}_7)\\
&\quad-2\boldsymbol{\sigma}_3\cdot(\boldsymbol{\sigma}_4\times\boldsymbol{\sigma}_6)+4\boldsymbol{\sigma}_3\cdot(\boldsymbol{\sigma}_5\times\boldsymbol{\sigma}_6)-2\boldsymbol{\sigma}_3\cdot(\boldsymbol{\sigma}_4\times\boldsymbol{\sigma}_7)+4\boldsymbol{\sigma}_3\cdot(\boldsymbol{\sigma}_4\times\boldsymbol{\sigma}_5\times\boldsymbol{\sigma}_6\times\boldsymbol{\sigma}_7)\\
&\quad-2\boldsymbol{\sigma}_2\cdot(\boldsymbol{\sigma}_3\times\boldsymbol{\sigma}_5\times\boldsymbol{\sigma}_6\times\boldsymbol{\sigma}_7)-2\boldsymbol{\sigma}_2\cdot(\boldsymbol{\sigma}_3\times\boldsymbol{\sigma}_4\times\boldsymbol{\sigma}_5\times\boldsymbol{\sigma}_7)-2\boldsymbol{\sigma}_1\cdot(\boldsymbol{\sigma}_3\times\boldsymbol{\sigma}_4\times\boldsymbol{\sigma}_5\times\boldsymbol{\sigma}_6)\\
&\quad-2\boldsymbol{\sigma}_1\cdot(\boldsymbol{\sigma}_2\times\boldsymbol{\sigma}_3\times\boldsymbol{\sigma}_5\times\boldsymbol{\sigma}_6)-2\boldsymbol{\sigma}_1\cdot(\boldsymbol{\sigma}_2\times\boldsymbol{\sigma}_3\times\boldsymbol{\sigma}_4\times\boldsymbol{\sigma}_5\times\boldsymbol{\sigma}_6\times\boldsymbol{\sigma}_7)\Big)\\
&\quad+\delta^4\Big(-2\boldsymbol{\sigma}_6\cdot\boldsymbol{\sigma}_7-8\boldsymbol{\sigma}_5\cdot\boldsymbol{\sigma}_7-2\boldsymbol{\sigma}_5\cdot\boldsymbol{\sigma}_6+2\boldsymbol{\sigma}_4\cdot\boldsymbol{\sigma}_7+2\boldsymbol{\sigma}_3\cdot\boldsymbol{\sigma}_6+2\boldsymbol{\sigma}_3\cdot\boldsymbol{\sigma}_7-2\boldsymbol{\sigma}_3\cdot(\boldsymbol{\sigma}_5\times\boldsymbol{\sigma}_6\times\boldsymbol{\sigma}_7)\\
&\quad+2\boldsymbol{\sigma}_3\cdot(\boldsymbol{\sigma}_4\times\boldsymbol{\sigma}_6\times\boldsymbol{\sigma}_7)-2\boldsymbol{\sigma}_3\cdot(\boldsymbol{\sigma}_4\times\boldsymbol{\sigma}_5\times\boldsymbol{\sigma}_7)+2\boldsymbol{\sigma}_2\cdot(\boldsymbol{\sigma}_3\times\boldsymbol{\sigma}_5\times\boldsymbol{\sigma}_7)+2\boldsymbol{\sigma}_1\cdot(\boldsymbol{\sigma}_3\times\boldsymbol{\sigma}_5\times\boldsymbol{\sigma}_6)\\
&\quad+2\boldsymbol{\sigma}_1\cdot(\boldsymbol{\sigma}_3\times\boldsymbol{\sigma}_4\times\boldsymbol{\sigma}_5\times\boldsymbol{\sigma}_6\times\boldsymbol{\sigma}_7)+2\boldsymbol{\sigma}_1\cdot(\boldsymbol{\sigma}_2\times\boldsymbol{\sigma}_3\times\boldsymbol{\sigma}_5\times\boldsymbol{\sigma}_6\times\boldsymbol{\sigma}_7)+2\boldsymbol{\sigma}_1\cdot(\boldsymbol{\sigma}_2\times\boldsymbol{\sigma}_3\times\boldsymbol{\sigma}_4\times\boldsymbol{\sigma}_5\times\boldsymbol{\sigma}_7)\Big)\\
&\quad+\delta^5\Big(4\boldsymbol{\sigma}_5\cdot(\boldsymbol{\sigma}_6\times\boldsymbol{\sigma}_7)-2\boldsymbol{\sigma}_3\cdot(\boldsymbol{\sigma}_6\times\boldsymbol{\sigma}_7)-2\boldsymbol{\sigma}_3\cdot(\boldsymbol{\sigma}_4\times\boldsymbol{\sigma}_7)-2\boldsymbol{\sigma}_1\cdot(\boldsymbol{\sigma}_3\times\boldsymbol{\sigma}_5\times\boldsymbol{\sigma}_6\times\boldsymbol{\sigma}_7)\\
&\quad-2\boldsymbol{\sigma}_1\cdot(\boldsymbol{\sigma}_3\times\boldsymbol{\sigma}_4\times\boldsymbol{\sigma}_5\times\boldsymbol{\sigma}_7)-2\boldsymbol{\sigma}_1\cdot(\boldsymbol{\sigma}_2\times\boldsymbol{\sigma}_3\times\boldsymbol{\sigma}_5\times\boldsymbol{\sigma}_7)\Big)\\
&\quad+\delta^6\Big(-4\boldsymbol{\sigma}_5\cdot\boldsymbol{\sigma}_7+2\boldsymbol{\sigma}_3\cdot\boldsymbol{\sigma}_7+2\boldsymbol{\sigma}_1\cdot(\boldsymbol{\sigma}_3\times\boldsymbol{\sigma}_5\times\boldsymbol{\sigma}_7)\Big)\,.
\end{aligned}
$$

Densities and charges are traceless.

Here $\boldsymbol{\sigma}_1\cdot(\boldsymbol{\sigma}_2\times\boldsymbol{\sigma}_3\times\cdots\times\boldsymbol{\sigma}_{\ell-1}\times\boldsymbol{\sigma}_\ell):=\boldsymbol{\sigma}_1\cdot(\boldsymbol{\sigma}_2\times(\boldsymbol{\sigma}_3\times(\cdots\times(\boldsymbol{\sigma}_{\ell-1}\times\boldsymbol{\sigma}_\ell)\cdots)))$

The R matrix $R_{ij}(\delta) = (\text{phase})e^{i\alpha(X_iX_j+Y_iY_j+Z_iZ_j)}$ can be implemented by elementary gates.

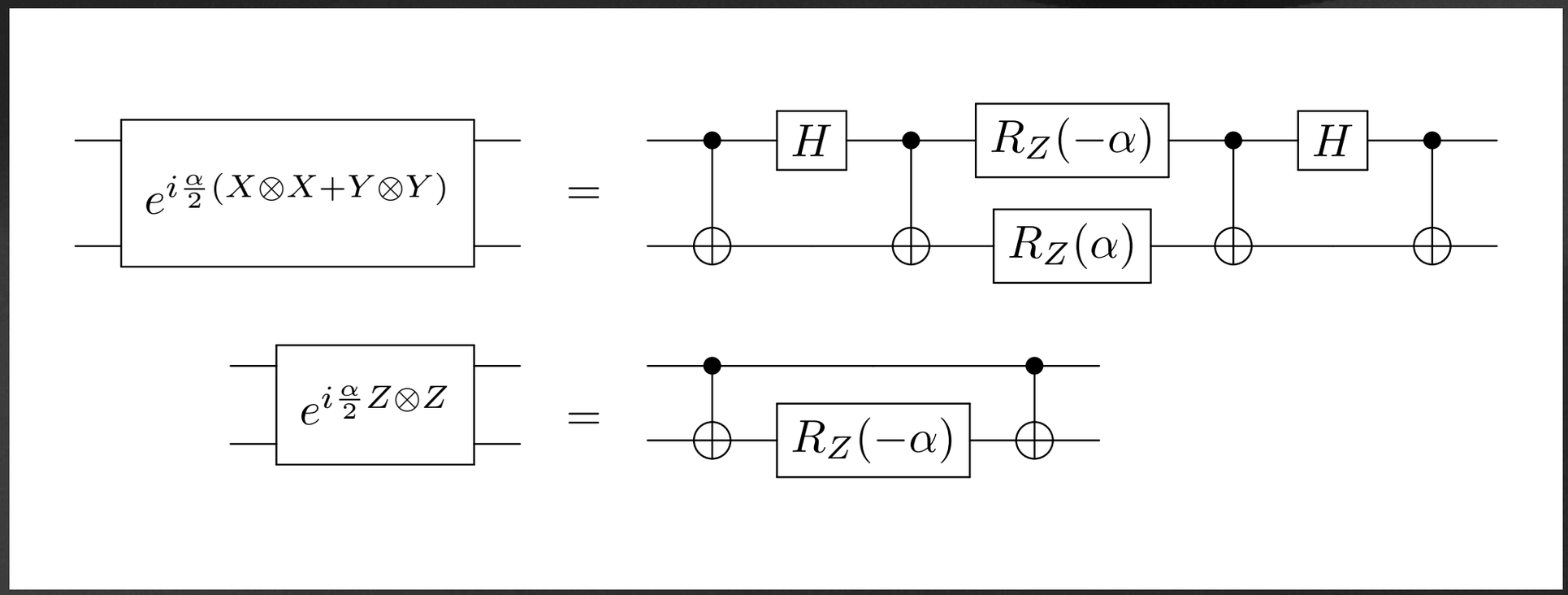

Quantum circuit

- Initialization: by default the quantum device prepares $|00\ldots0\rangle$. We further apply some of H, S, and Pauli gates (X, Y, and Z) to prepare a simultaneous eigenstate $|s_1\ldots s_N\rangle_{P_1\ldots P_N}$ of $P_i \in \{X, Y, Z\}$ with eigenvalues $(-1)^{s_i}$.

- Time evolution: d repetitions of

$$\mathcal{U}(\delta) = \left(\prod_{j=1}^{N/2} R_{2j-1,2j}(\delta)\right)\left(\prod_{j=1}^{N/2} R_{2j,2j+1}(\delta)\right).$$

- Measurement: we measure the eigenvalue of X, Y, or Z for each qubit.

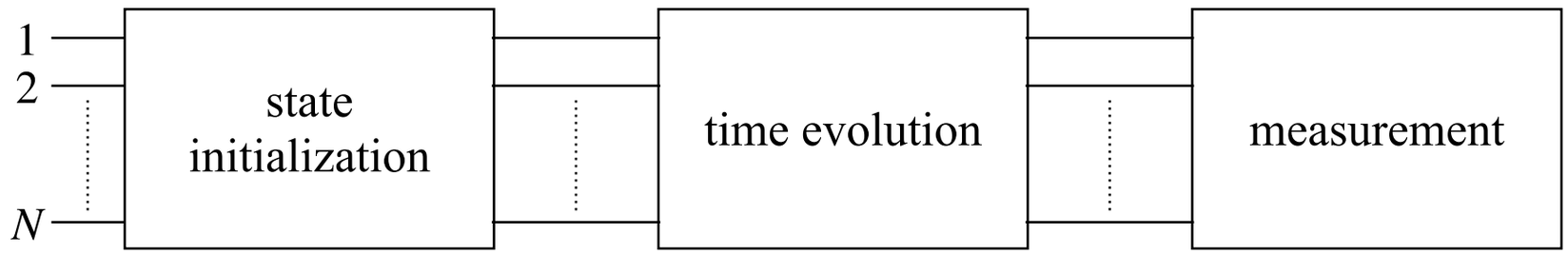

Estimating observables

- One can compute (estimate) the expectation value of a charge

$$Q = \sum_{P \in \{I,X,Y,Z\}^{\otimes N}} c_{Q,P} P, \quad c_{Q,P} \in \mathbb{C},$$

  from the measurement results in various measurement bases.

Quantum devices

IBM: Superconducting devices

- Superconducting transmon qubits made of materials such as niobium and aluminum placed on a silicon chip. Two energy-levels form an approximate qubit.

- We obtained access to the devices through the University of Tokyo. (Supported by UTokyo Quantum Initiative).

- We used the ibm_kawasaki (27-qubit, before upgrade) and ibm_washington (127-qubit) processors.

source: https://japan.zdnet.com/article/35174399/

IonQ: trapped ion devices

- We mainly used IonQ's older device called Harmony. (There is a newer device called Aria.)
- A linear chain of $^{171}\mathrm{Yb}^{+}$ ions near an electrode trap.
- 11 qubits with all-to-all couplings.
- We got indirect access through Google Cloud and direct access through IonQ itself.

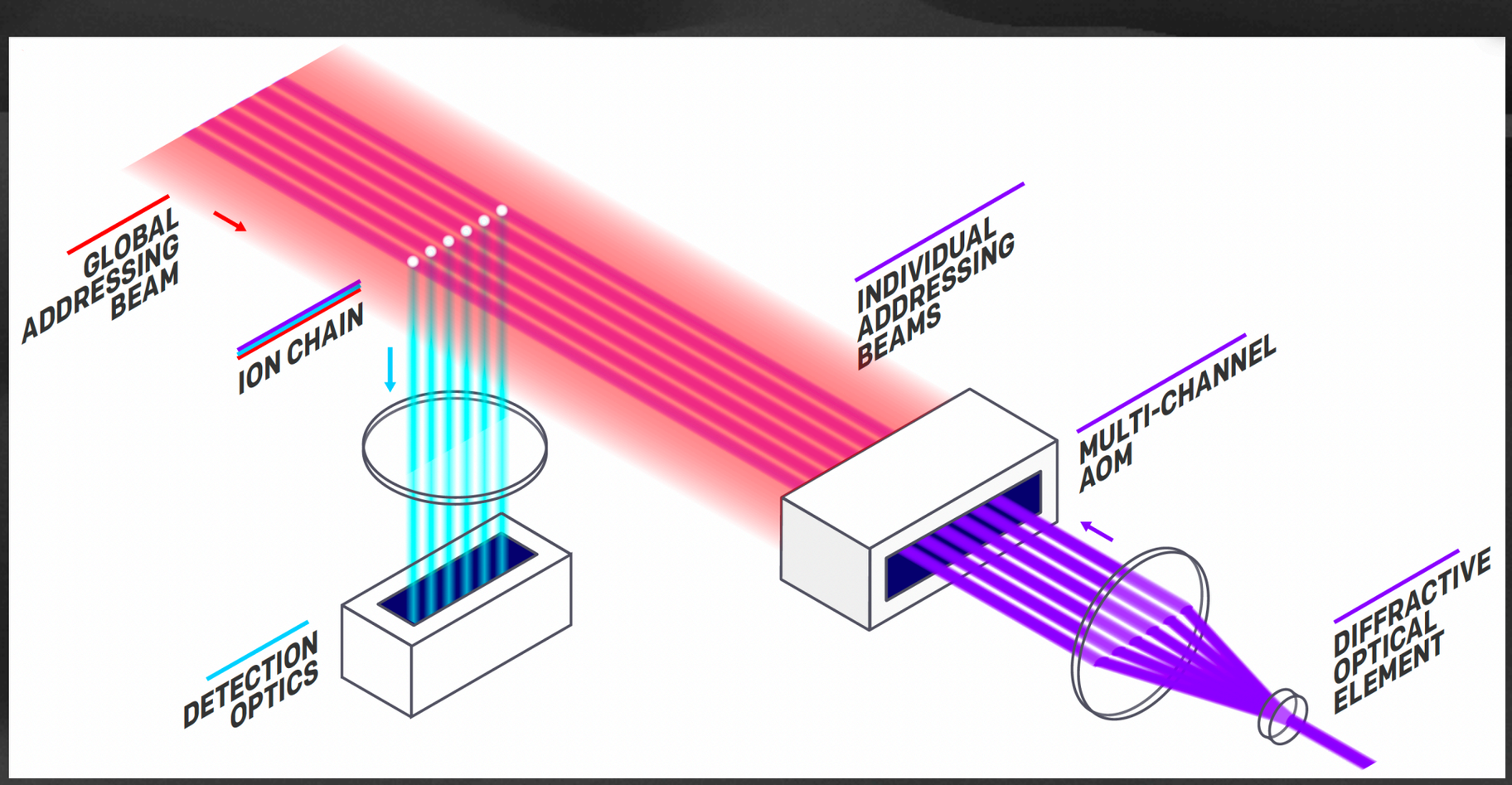

arXiv:1903.08181

Results of real-device simulations

Simulation results for ibm_kawasaki

- $\langle Q_1^+ \rangle = \mathrm{tr}(\rho Q_1^+)$ **decays exponentially** to zero asymptotically, **due to noise**. No error mitigation.
- Error bars are hidden by markers. Rescaled for better visibility. The theoretical values are shown by dotted lines. Fit by $c_1 e^{-\gamma d} + c_2$.
- The initial state is $|0101\ldots01\rangle$.
- Large fluctuations from one step to the next (most likely due to change in device parameters).

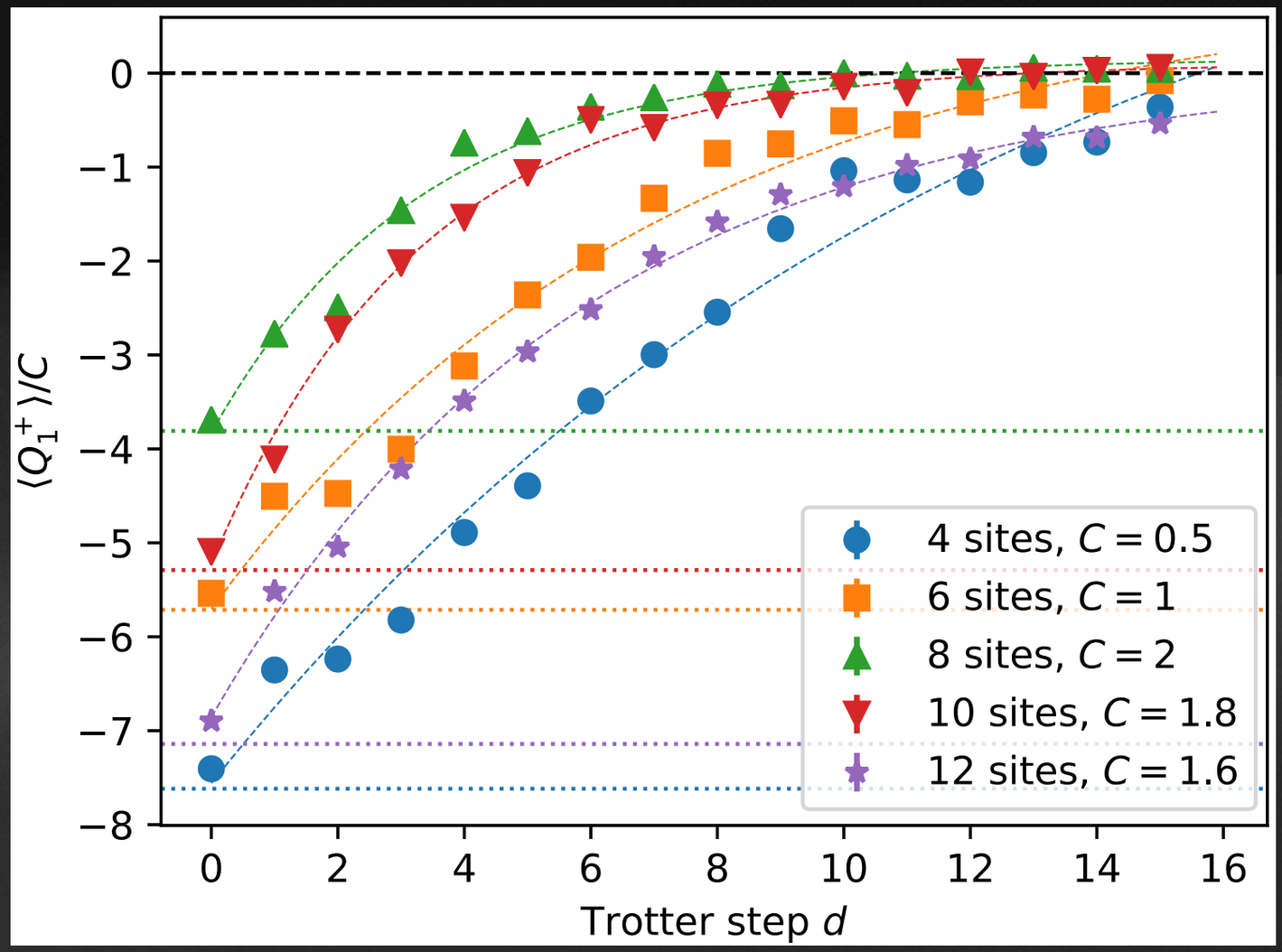

Only the 12-site simulation is for a circular topology.

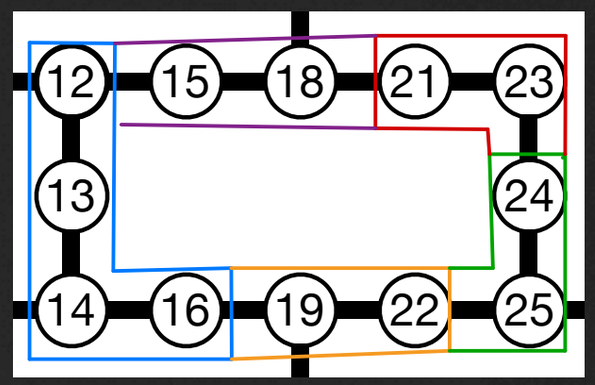

- Similar results for $Q_1^{\mathrm{dif}} = [Q_1^+(\delta) - Q_1^-(\delta)]/2$.
- The initial states are chosen appropriately to give non-zero theoretical expectation values.

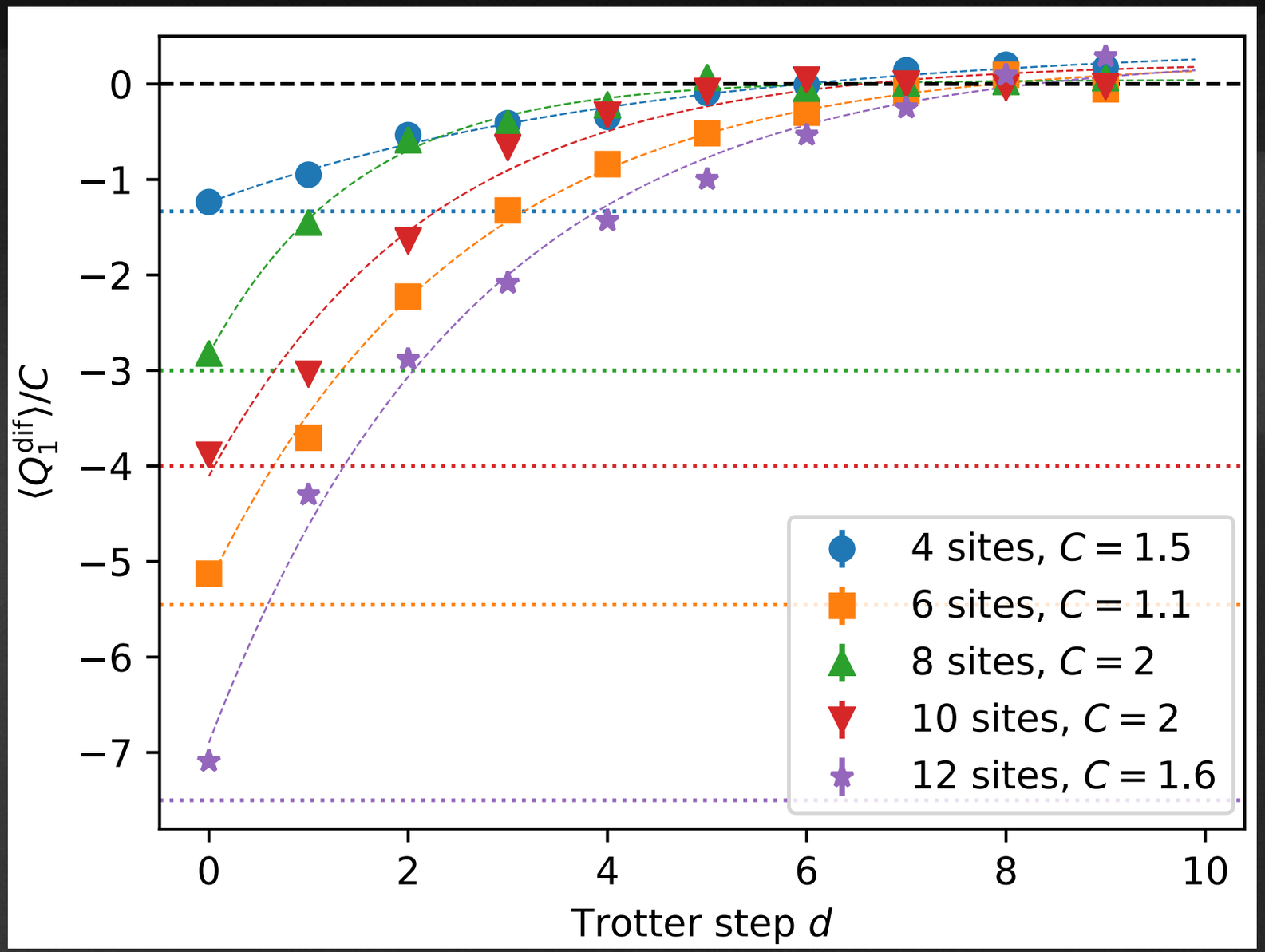

Simulations on a 127-qubit IBM device

- Quantum device ibm_washington with 127 qubits.
- We ran simulations with qubits on loops of size 12, 20, and 84. The 84-qubit loop is shown in the figure.
- To have slower decays, it is important to avoid faulty (purple) qubits and connections.

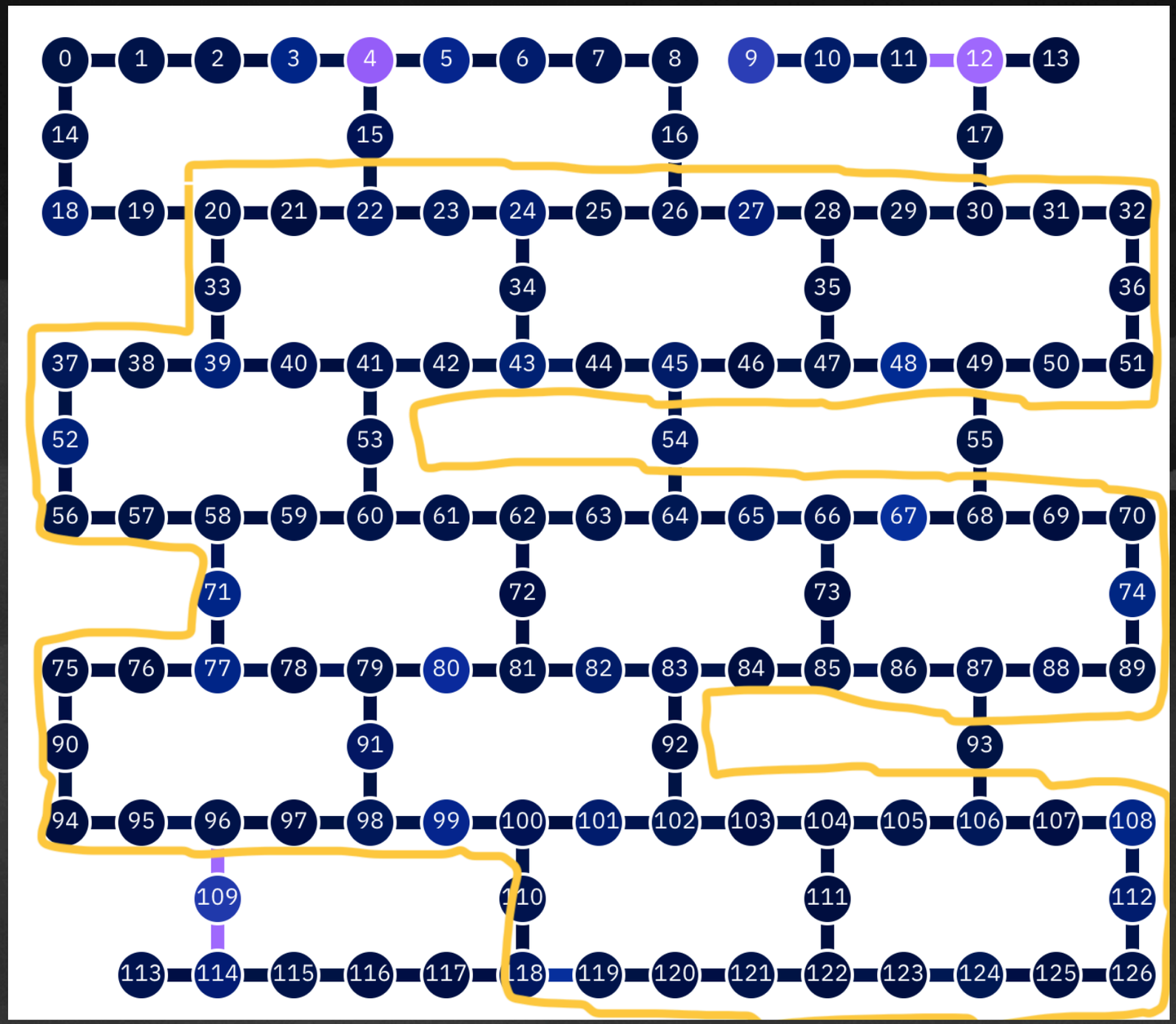

Simulation results on large chains

- Loops of size 12, 20, and 84.
- Similar exponential decays of $\langle Q_1^+ \rangle$.
- For the 84-site run, we had 10^6 shots (circuit executions) for each value of d.
- (There were significant time gaps between some data.)

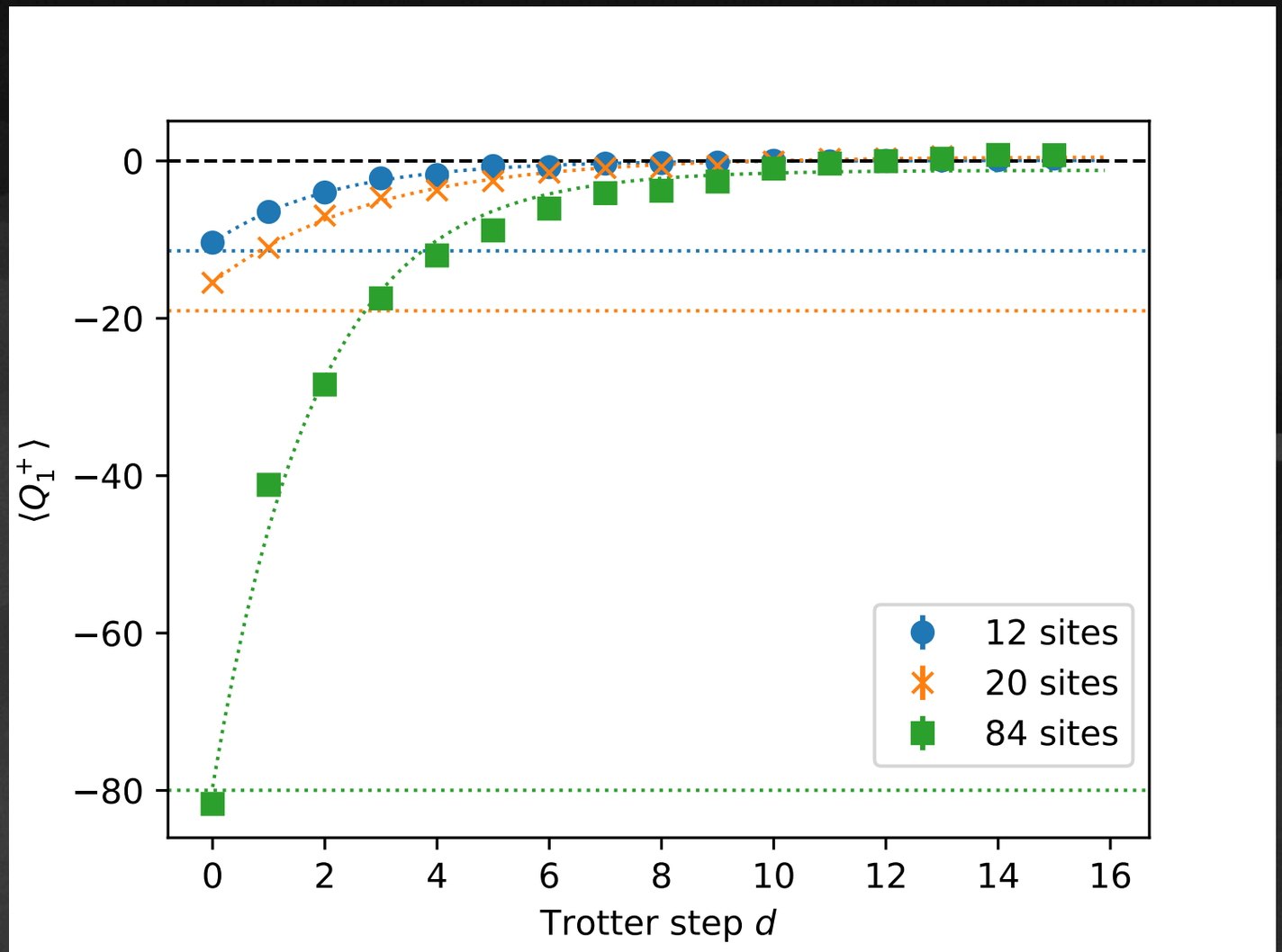

Simulation results for IonQ Harmony

- Similar exponential decays.
- To have slower decays, it seems important to use the qubits (ions) in the middle of the linear chain.

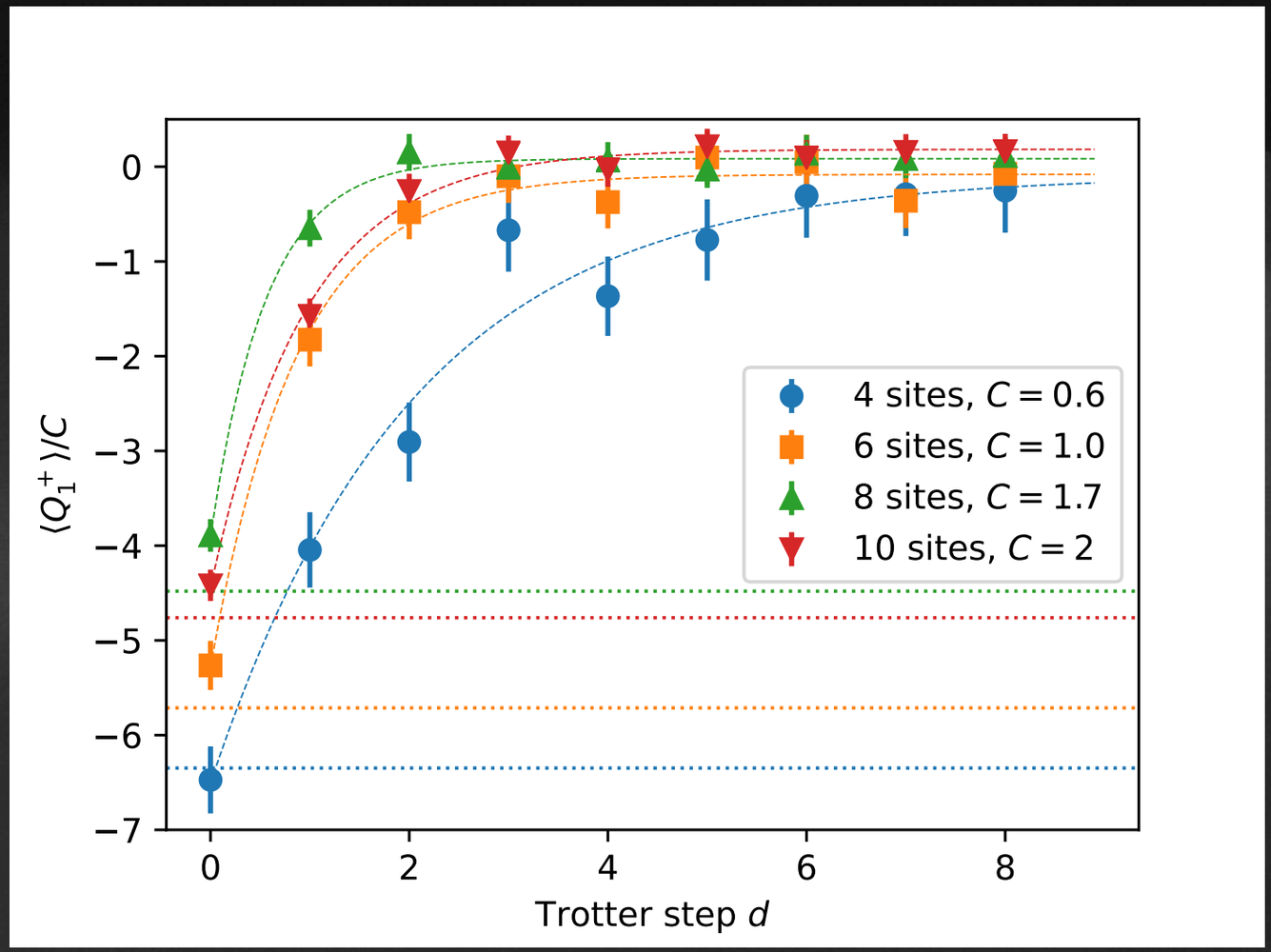

Emulator results and theoretical analysis

Numerical noise models

- We ran digital quantum simulations on the Qiskit (classical) simulator with noise models.
- We considered two noise models:
  1. (1-qubit) depolarizing error channels inserted after 1- and 2-qubit gate operations.
  2. (1-qubit) amplitude-and-phase damping error channels inserted after 1- and 2-qubit gate operations.

Classical emulation of quantum simulation with a depolarizing noise model

- $\Phi_{\text{depo}}(\rho) = \sum_{j=1}^{4} D_j \rho D_j^\dagger$ with

$$D_1 = \sqrt{1 - \frac{3p}{4}}\, I, \quad D_2 = \sqrt{\frac{p}{4}}\, X,$$

$$D_3 = \sqrt{\frac{p}{4}}\, Y, \quad D_4 = \sqrt{\frac{p}{4}}\, Z$$

inserted after gate operations.

- $\langle Q_j^+ \rangle$ and $\langle Q_j^{\text{dif}} \rangle$ decay exponentially to zero. This suggests that the finite state is completely mixed.

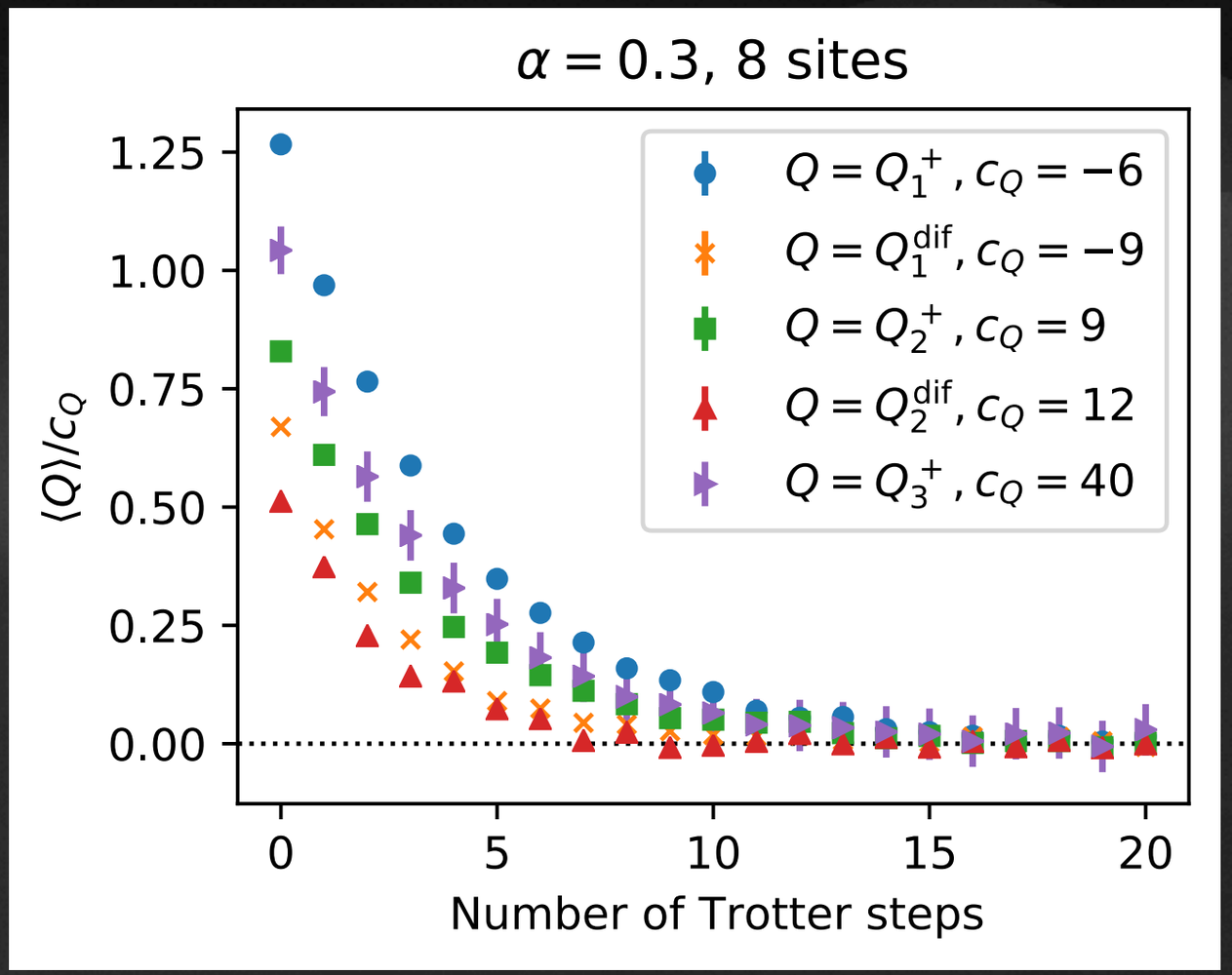

Classical emulation of quantum simulation with a amplitude-and-phase damping noise model

- $\Phi_{\text{damp}}(\rho) = \sum_{j=1}^{3} D_j \rho D_j^\dagger$ with

$$D_1 = \begin{pmatrix} 1 & 0 \\ 0 & \sqrt{1-\lambda_a-\lambda_p} \end{pmatrix},$$

$$D_2 = \begin{pmatrix} 0 & \sqrt{\lambda_a} \\ 0 & 0 \end{pmatrix}, \quad D_3 = \begin{pmatrix} 0 & 0 \\ 0 & \sqrt{\lambda_p} \end{pmatrix}$$

inserted after gate operations.

- $\langle Q_j^+ \rangle$ (and $\langle Q_j^{\text{dif}} \rangle$) asymptote to finite values. The finite state is unique and is NOT completely mixed. Checked by quantum tomography.

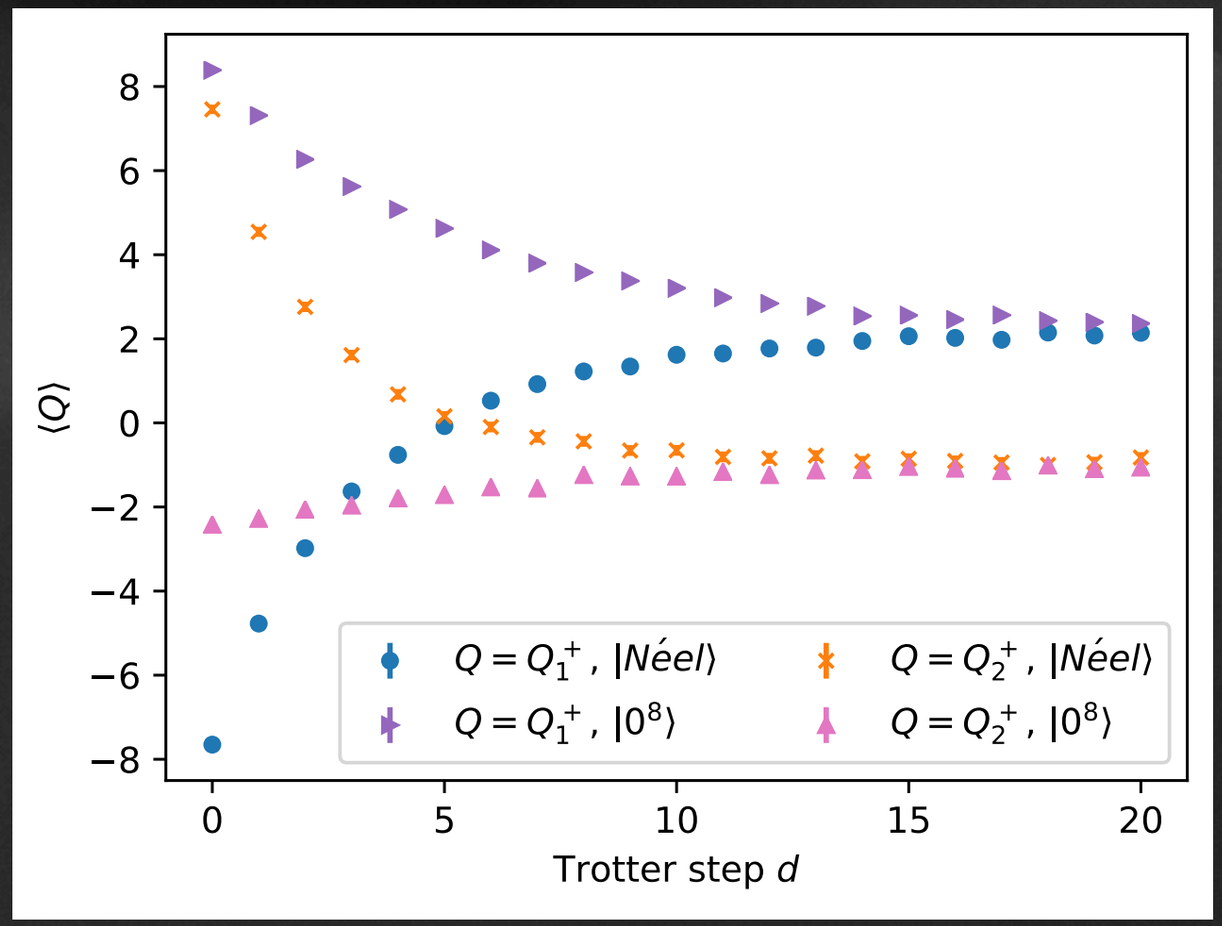

Analysis fo quantum channels

- The initial state $\rho_0 = \ \psi_0\rangle\langle\psi_0\ $ is mapped, at Trotter step d, to $\Phi^d(\rho)$, where Φ is a noisy time evolution for a single step.
- The expectation value of a conserved charge Q at step d is $\langle Q\rangle_d = \mathrm{tr}[\Phi^d(\rho)Q]$.
- We studied the eigenvalue distribution of the linear map $\rho \to \Phi(\rho)$.

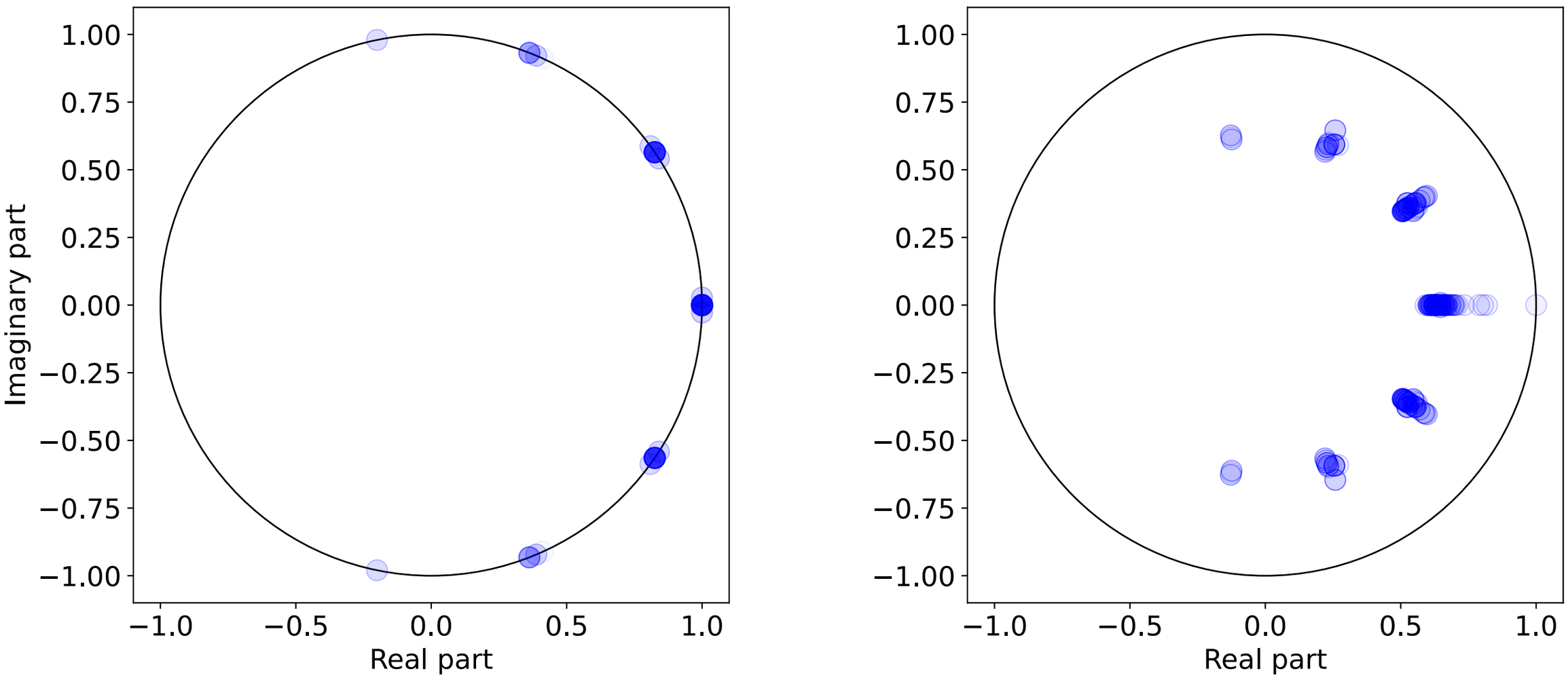

- The eigenvalues for the single time step Φ on 4 sites.
- In the noiseless case, the evolution is unitary and the eigenvalues are on a unit circle.
- In the depolarizing noise model, all the eigenvalues except one are strictly inside the unit circle. There remains a single eigenvalue 1, corresponding to the unique fixed point (completely mixed state) of Φ.

Possible use of conserved charges as benchmarks for future quantum computing

- For future quantum devices we expect smaller error rates. We propose to use the higher conserved charges of the integrable Trotterization as benchmarks.

- On a classical simulator, we numerically computed the time evolution on 8 sites.

- The slopes of early-tiime decays depend on the types and the degrees of the charges.

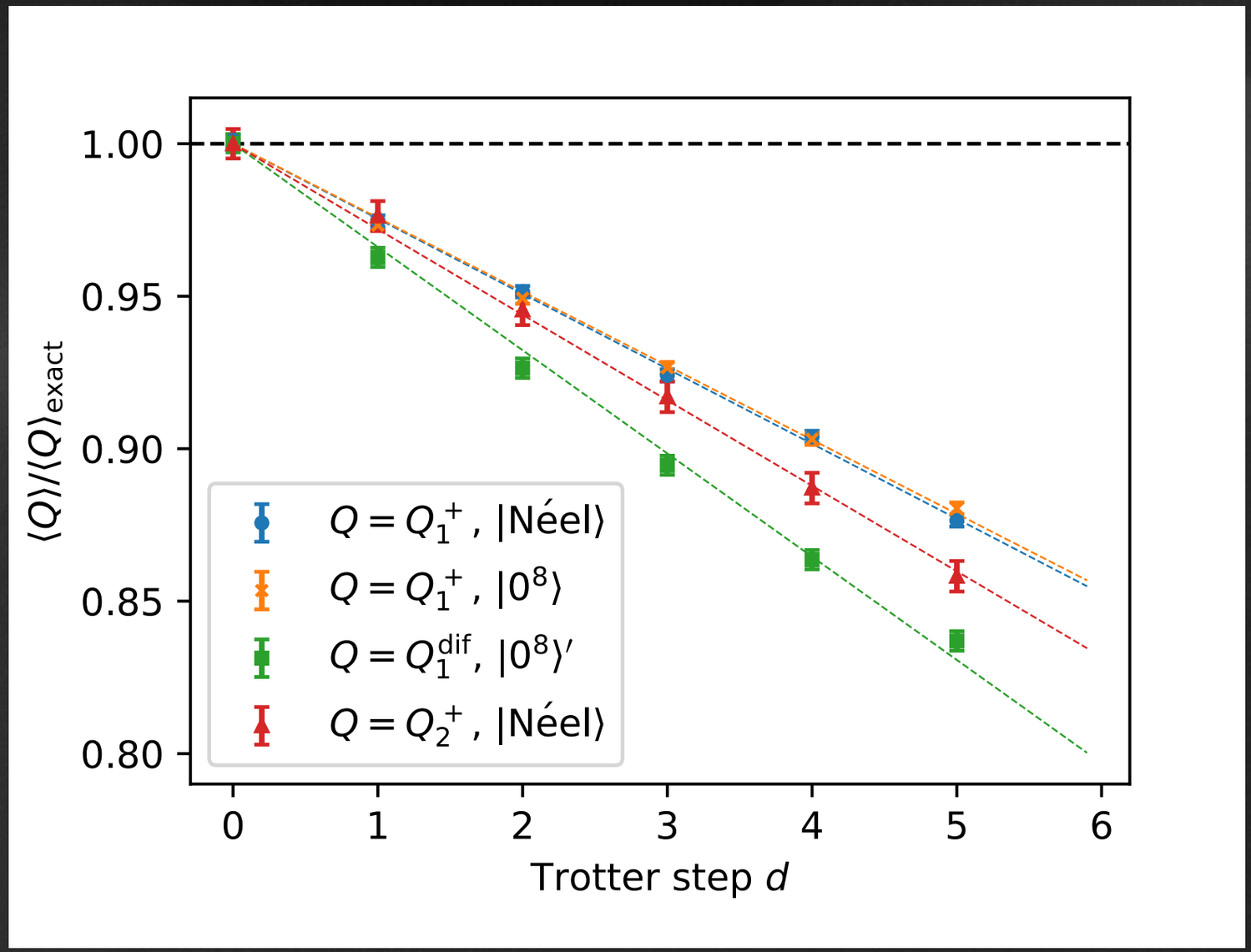

Summary

- We implemented the integrable Trotterization of the Heisenberg spin 1/2 XXX spin chain on real quantum computers and on classical simulators. We used superconducting devices of IBM and trapped ion devices of IonQ.

- As expected, conserved charges decay due to noise on the current quantum devices.

- The early-time decay rate seems to depend on the type and the degree of the charge. Higher charges are candidates of benchmarks for the future quantum simulation.

Future directions

- With H. Sukeno, we proposed a measurement-based scheme for quantum-simulating abelian lattice gauge theories in SciPost Phys. 14, 129 (2023). This involves preparing a cluster state first and then performing adaptive measurements.

- When measurements can be performed more efficiently than entangling gates, the measurement-based scheme may be faster than the circuit-based scheme.

- I’m hoping to implement the measurement-based quantum simulation on a real device with mid-circuit measurement capabilities (in a couple of years).

Back-up slides

More details on devices

- $\alpha = 0.3$
- ibm_kawasaki:
  - 27 qubits, QV=unknown, Falcon r5.11.
  - 90K shots per step for the 4-site simulation.
- ibm_washington: 127 qubits, QV=64, Eagle r1.
- IonQ
  - Uses the Sorenen-Molmer 2-qubit gate.
  - 2.3K shots per step for the 4-site simulation.

Transmon

From Wikipedia, the free encyclopedia

In quantum computing, and more specifically in superconducting quantum computing, a **transmon** is a type of superconducting charge qubit that was designed to have reduced sensitivity to charge noise. The transmon was developed by Robert J. Schoelkopf, Michel Devoret, Steven M. Girvin, and their colleagues at Yale University in 2007.[1][2] Its name is an abbreviation of the term *transmission line shunted plasma oscillation qubit*; one which consists of a Cooper-pair box "where the two superconductors are also capacitatively shunted in order to decrease the sensitivity to charge noise, while maintaining a sufficient anharmonicity for selective qubit control".[3]

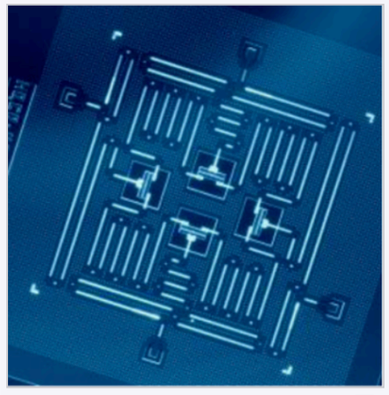

A device consisting of four transmon qubits, four quantum buses, and four readout resonators fabricated by IBM and published in *npj Quantum Information* in January 2017.[4]

The transmon achieves its reduced sensitivity to charge noise by significantly increasing the ratio of the Josephson energy to the charging energy. This is accomplished through the use of a large shunting capacitor. The result is energy level spacings that are approximately independent of offset charge. Planar on-chip transmon qubits have T_1 coherence times ~ 30 μs to 40 μs.[5] By replacing the superconducting transmission line cavity with a three-dimensional superconducting cavity, recent work on transmon qubits has shown significantly improved T_1 times, as long as 95 μs.[6][7] These results demonstrate that previous T_1 times were not limited by Josephson junction losses. Understanding the fundamental limits on the coherence time in superconducting qubits such as the transmon is an active area of research.

Comparison to Cooper-pair box [edit]

The transmon design is similar to the first design of the charge qubit[8] known as a "Cooper-pair box", both are described by the same Hamiltonian, with the only difference being the increase in the $E_\mathrm{J}/E_\mathrm{C}$ ratio, achieved by shunting the Josephson junction with an additional large capacitor. Here E_J is the Josephson energy of the junction, and E_C is the charging energy inversely proportional to the total capacitance of the qubit circuit. The benefit of increasing the $E_\mathrm{J}/E_\mathrm{C}$ ratio is insensitivity to charge noise - the energy levels become independent of electrical charge across the junction, thus the coherence times of the qubit are prolonged. The disadvantage is decrease in the anharmonicity $\frac{(E_2 - E_1) - (E_1 - E_0)}{E_1 - E_0}$, where E_i is the energy of the state $|i\rangle$. Reduced anharmonicity complicates the device operation as a two level system, e.g. exciting the device from the ground state to the first excited state by a resonant pulse also populates the second excited state. This complication is overcome by complex microwave pulse design, that takes into account the higher energy levels, and prohibits their excitation by destructive interference.

Measurement, control and coupling of the transmons is performed by means of microwave resonators with techniques of circuit quantum electrodynamics, also applicable to other superconducting qubits. The coupling to the resonators is done by putting a capacitor between the qubit and the resonator, at a point where the resonator electromagnetic field is biggest. For example, in IBM Quantum Experience devices, the resonators are implemented with "quarter wave" coplanar waveguide with maximal field at the signal-ground short at the waveguide end, thus every IBM transmon qubit has a long resonator "tail". The initial proposal included similar transmission line resonators coupled to every transmon, becoming a part of the name. However,

Part of a series of articles about
Quantum mechanics
$i\hbar\frac{\partial}{\partial t}|\psi(t)\rangle = \hat{H}|\psi(t)\rangle$
Schrödinger equation

Introduction · **Glossary** · **History**

Background [show]
Fundamentals [show]
Experiments [show]
Formulations [show]
Equations [show]
Interpretations [show]
Advanced topics [show]
Scientists [show]

V • T • E